IEEE Access
Multidisciplinary | Rapid Review | Open Access Journal

Received May 10, 2020, accepted July 17, 2020, date of publication July 29, 2020, date of current version August 10, 2020.

Digital Object Identifier 10.1109/ACCESS.2020.3012657

Physically Based Analytical Model of Heavily Doped Silicon Wafers Based Proposed Solar Cell Microstructure

MARWA S. SALEM[1,2], ABDULLAH J. ALZAHRANI[1], RABIE A. RAMADAN[1,3], (Member, IEEE), ADWAN ALANAZI[1], AHMED SHAKER[4], MOHAMED ABOUELATTA[5], CHRISTIAN GONTRAND[6,7], MOHAMMED ELBANNA[4], AND ABDELHALIM ZEKRY[5]

[1]Department of Computer Engineering, College of Computer Science and Engineering, University of Ha'il, Ha'il 2440, Saudi Arabia
[2]Department of Electrical Communication and Electronics Systems Engineering, Faculty of Engineering, Modern Science and Arts University, Cairo 12585, Egypt
[3]Department of Computer Engineering, Faculty of Engineering, Cairo University, Cairo 12613, Egypt
[4]Department of Engineering Physics and Mathematics, Faculty of Engineering, Ain Shams University, Cairo 11517, Egypt
[5]Department of Electronics and Communications, Faculty of Engineering, Ain Shams University, Cairo 11517, Egypt
[6]INSA Lyon, 69621 Villeurbanne, France
[7]IEP, INSA, Université Euro-méditerranéenne de Fès, 30000 Fez, Morocco

Corresponding author: Rabie A. Ramadan (rabie@rabieramadan.org)

This work was supported the Deanship of Scientific Research at the University of Hail under Research Group Project number : RG-191279.

ABSTRACT In this paper, an analytical model of a proposed low-cost high efficiency NPN silicon-based solar cell structure is presented. The structure is based on using low cost heavily doped commercially available silicon wafers and proposed to be fabricated by the same steps as the conventional solar cells except an extra deep trench etch step. Moreover, the cell has been engineered to react to the UV spectrum, resulting in a greater conversion performance. The presented analytical model takes the electrical and optical characteristics into account. Thus, the influence of both physical and technological parameters on the structure performance could be easily examined. Consequently, the optimization of the structure performance becomes visible. To inspect the validity of the analytical model, a comparison of the main performance parameters resulting from the model results with TCAD simulations is carried out, showing good agreement.

INDEX TERMS Low cost, high efficiency, high-doped wafers, solar cell, analytical model.

I. INTRODUCTION

Recently, thin film solar cells have been presented as competitors to the single crystal silicon solar cells due to their low cost and their rapid efficiency improvement [1]. However, thin film solar cells technology has some limitations like the difficulty of absorbing longer wavelengths of the light spectrum due to their small thickness of the active layer [2], toxic materials involved and stability issues [3]. So, this technology still requires more research before it can be made commercially available. Accordingly, silicon is still the main material used in PV applications due to efficient, reliable and stable solar cells produced from silicon. Actually, silicon-based solar cell technology constitutes about 90% of the solar PV market due to the intensive efforts being led by the microelectronic industry. However, the cost of the high efficiency planar solar cell is still high and much more expensive than the thin film technologies [4], [5].

The associate editor coordinating the review of this manuscript and approving it for publication was Huiqing Wen.

Still, few research works have been done to fabricate silicon-based solar cells in a cheap way with relatively high efficiency [6]–[9]. One of the most interesting attempts to get high efficiency low cost silicon-based cells is to use a nanorod with a high-doped pn junction in the radial direction [10], [11]. The visibility of this nanorod solar cell involves creating a dense array of well-oriented nanorods, each with a pn junction, which is difficult to be fabricated. Efforts are still in progress to raise efficiency while keeping low-cost cells to meet the high demand of the industry [12], [13].

In order to produce low-cost solar cells, a low-cost substrate may be used. However, using these inexpensive absorbers results in a high density of defects or a large degree of impurity. This, in turn, reduces the diffusion length of the low minority carrier [14], [15]. Using such low diffusion length materials as the base of planar solar cell limits carrier collection by minority carrier diffusion. As a result, the cell performance is degraded. The solution to such a problem is achieved by generating electron-hole

pairs from light absorption vertically and collecting them laterally. Thus, the diffusion length can be decreased without deteriorating the performance of the cell. This concept paves the way for the usage of low-quality and low-cost with high-doped silicon wafers in solar cells as previously demonstrated by TCAD simulation [13].

Analytical models are vital to understanding the underlined physics of the device behavior. Using analytical models in the optimization of the device parameters to obtain the best performance is recommended vs TCAD simulation as the latter requires long times to be performed. Many analytical models developed for various types of solar cells are found in the literature [16]. In [10], an analytical model for the radial p-n junction nanorod structure was developed, and an efficiency of up to 11% was obtained. In [17], an analytical model, based on Green's function theory, was used to calculate the main p-n and p-i-n radial solar cells device performance parameters.

The npn cell, presented in this work, is based on a proposed low-cost solar cell structure, which was previously published by our research group [13]. TCAD simulations of that cell give less than 15%. According to recent studies [18], [19], the efficiencies of the majority modules are in the range from 10% to 17% according to the physical dimensions and the manufacturer. Few modules are of efficiency above 22% [19]. Although our npn cell efficiency is still low compared to other commercial silicon solar cells, we believe that the optimization of such npn cell could result in achieving relatively higher efficiencies.

In this paper, a physically based analytical model for the proposed npn solar cell structure, is presented. To interpret the essence of device operation, device simulations using this model are performed. The simulation is analyzed firstly in terms of the illuminated IV characteristics. The open-circuit voltage (V_{oc}), short circuit current density (J_{sc}), fill factor (FF), and conversion efficiency (η_c) are calculated. Additionally, the optical performance is presented regarding the quantum efficiency and spectral response. The influence of both physical and technological parameters on the structure performance is examined. A comparison between the model results and TCAD simulation results is carried out, showing good agreement.

The paper is organized as follows. Section 2 outlines the proposed efficient heavily doped silicon solar cell structure and its main physics. Section 3 presents the analytical model of the structure. It is considered as two independent solar cells: vertical and horizontal. Section 4 addresses a comparison of the analytical model implemented in MATLAB vs. SILVACO TCAD device simulations. Finally, a summary of the important findings and conclusions of this work is offered in Section 5.

II. PROPOSED HEAVILY DOPED SILICON SOLAR CELL STRUCTURE

A 3D view of the proposed structure of the solar cell is shown in Figure 1. The contacts are taken from the side and bottom

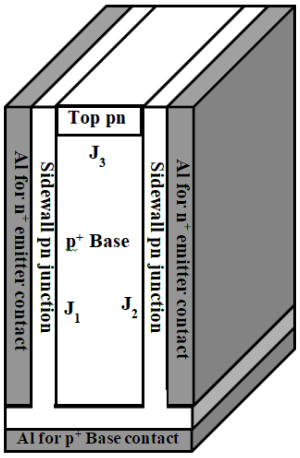

FIGURE 1. Three-dimensional npn solar cell layout view displaying the three different pn junctions.

of the structure. The bottom contact is Aluminum (Al) base contact which is considered the anode while the cathode is taken from both sides (Al emitter contact).

To have a solar cell structure based on vertical generation and lateral collection of light generated carriers, the utilized wafer in this structure has to be etched vertically on regular distances to produce deep trenches. Then, an n^+ region is added to form a side wall pn junction. This junction is responsible for the lateral collection of vertically light-generated carriers regarding high doping and low diffusion length, as in the case of low-cost highly doped silicon wafers. It collects the generated carriers from the long wavelength solar radiation spectrum. The top n^+ region in this system is working as an ultraviolet collector [13]. Therefore, the structure collects both the ultraviolet generated carriers as well as the generated carriers from the long wavelength solar radiation spectrum.

There are many advantages of using a structure with two sidewall pn junctions, npn structure [12]. Its main advantage is that it collects the light generated carriers from two sides (by using two sidewall pn junctions). Thus, its base width is double the base width of the structure when compared with only one sidewall pn junction. The double size of the base width of the npn structure often raises the active area in comparison to the shadowing area which, in effect, contributes to better illumination. Consequently, the short circuit current density increases and thus, the efficiency improves. The closed notches shown in Fig. 1 have an advantage of facilitating the connection of the metal tracks for the n^+ emitter contact in the final wafer mask, as it is mainly used for n^+ emitter contact. Also, the aluminum series resistance is reduced, which enhances the npn structure fill factor.

Commercially speaking, the npn is a low-cost structure. This is because it is etched through a commercially available, highly doped silicon wafer [20], [21]. Besides, it is designed

to respond to the ultraviolet part of the solar radiation spectrum. It could collect the ultraviolet part by optimizing both the doping and thickness of the top pn junction. Also, the proposed npn structure needs straight forward fabrication processes. Thus, no extra cost is needed for fabrication.

III. ANALYTICAL MODEL FOR THE NPN SOLAR CELL STRUCTURE

The main advantage of building up an analytical model, for any structure or device, is that it gives a transparent solution. Therefore, the influence of both physical and technological parameters on the device performance can be examined quickly and simply. Additionally, analytical models enable the estimation of minimum, nominal, and maximum values for device parameters. Thus, one can have a good picture of how to enhance the device performance before going through the complicated exact solutions of device simulators.

In this section, the superposition principle is used to get the complete model of the structure behavior. The electrical model is built up for both the sidewall and top pn junctions of the npn structure. Then, the optical model, which describes how to include the input solar radiation spectrum into the analytical model, is presented.

A. SUPERPOSITION PRINCIPLE FOR MODELING THE OVERALL PERFORMANCE OF THE NPN STRUCTURE

In the analytical model, the npn structure, as illustrated in Fig. 1, is assumed to have three pn junctions: one top and two sidewall junctions. There are two types of collection for light generated carriers inside this structure, the lateral collection, caused by the two vertical pn junctions (J_1 and J_2), and the vertical collection caused by the top planar pn junction (J_3). The top pn junction is beneficial for the selection of photogenerated electron-hole pairs through the ultraviolet component of the incident solar radiation. The vertical sidewall pn junctions J_1 and J_2 are considered the main core of the structure. They are responsible for the lateral collection of the vertically light generated carriers caused by longer wavelength photons through low diffusion length. These two vertical junctions are the solution for overcoming the problem of using highly doped silicon with low diffusion length in the conventional planar solar cell.

To include both vertical and horizontal junctions in the analytical model, they are treated as two independent solar cells. The vertical solar cell consists of J_1 and J_2, and horizontal solar cell consists of J_3. The analytical model is carried out for each one of them for both dark and short circuit illumination case. The overall structure performance is the superposition of the two-part cell performance. The top pn junction is a planar solar cell and the analytical model of such a cell is well established [22], [23]. So, the analytical model is carried only for the vertical junctions J_1 and J_2.

In the electrical analytical model, care is oriented only towards photons that pass and be absorbed through the structure. These photons are responsible for the light generated electron-hole pairs, excess carriers. Excess carriers are diffused, causing current flow inside the solar cell, and, eventually, they control its operation. Thus, it is important to model excess carriers in the electrical model to be able to model solar cell electrical performance, the current flow inside the cell and, hence, its IV characteristics.

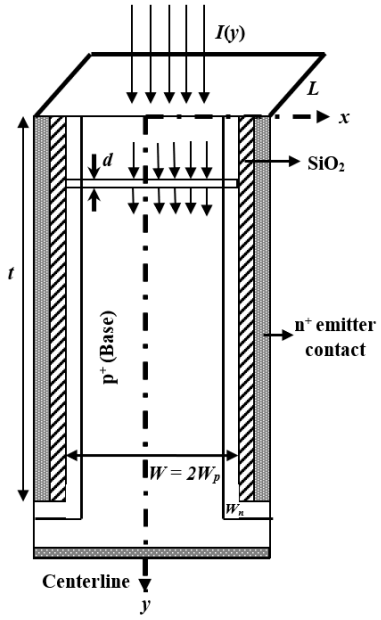

FIGURE 2. The npn structure with a detailed description of its parameters.

Fig. 2 shows the npn structure with more parameters' details. It should be pointed out here that the deposition of aluminum directly on the sidewall junction to take the cathode contact is not recommended as the Ohmic contact has nearly infinite surface recombination velocity which contributes in the recombination of the light generated carriers. So, passivation of the sidewall surfaces with clean SiO_2 oxide is recommended as shown in the figure. The different parameters are identified in Table 1 where $I(y)$ represent the photon flux. The drift-diffusion model is used to get the current components in both n^+ emitter and p^+ base regions. This is done for both short circuit and dark cases. From Fig. 2, as the structure has symmetry, the centerline is taken at its center to simplify the solution. Thus, the solution can be carried out for half the structure then the current is multiplied by two. The incident solar radiation is assumed to be perpendicular to the structure.

Using the one-dimensional drift diffusion model, the electron current density is determined from the following,

$$J_n = q\mu_n E + qD_n \frac{\delta \Delta n}{\delta x} \tag{1}$$

where q, μ_n, D_n and E are the electron charge, electron mobility, electron diffusion constant and electric field, respectively.$\Delta\ n$ is being the excess electron concentration. The continuity equation at steady state is used as follows:

$$\frac{1}{q}\frac{\delta J_n}{\delta x} - U + g_{ph}(y, \lambda) = 0 \tag{2}$$

TABLE 1. Main parameters of the npn solar cell structure.

Parameter	Description
N_{p+}	p^+ base doping
W_p	p^+ Base width
$W = 2W_p$	Cell base width
W_{n+}	Top n^+ Thickness
$N_{n,\text{top}}$	Top n^+ Doping
W_n	Emitter width
N_E	Emitter Doping
t	Cell thickness
L	Structure length in the z-direction
$I(y)$	Photons flux

where $U = \frac{\Delta n}{\tau_n}$ and Δn is the excess electron concentration. The electron lifetime, τ_n, includes both the Shockley Read Hall and auger recombination. Auger recombination is important in this case as the doping of p^+ base is high. From equations (2) and (1), the continuity equation in terms of L_n becomes:

$$\frac{\delta^2 \Delta n}{\delta x^2} - \frac{\Delta n}{L_n^2} + \tau_n g_{ph}(y, \lambda) = 0 \tag{3}$$

where L_n is the electron diffusion length that is found from,

$$L_n^2 = D_n \tau_n \tag{4}$$

Similarly, for holes:

$$\frac{\delta^2 \Delta p}{\delta x^2} - \frac{\Delta p}{L_p^2} + \tau_p g_{ph}(y, \lambda) = 0 \tag{5}$$

where Δp is the excess hole concentration and τ_p is the hole lifetime. The hole diffusion length L_p is related to the hole diffusion constant (D_p) and its lifetime as,

$$L_p^2 = D_p \tau_p \tag{6}$$

1) DERIVATION OF EXCESS CARRIERS' CONCENTRATIONS IN SHORT CIRCUIT CASE

Excess carriers' concentration and current densities in short circuit case are derived firstly for p^+ base region then for n+ emitter region, sidewall pn junction. Fig. 3 shows the distribution of excess carriers inside the three quasi neutral regions of the structure; two n^+ emitters, J_1 and J_2, the p^+ base region. It also shows excess carriers' distribution in the two depletion regions of J_1 and J_2 in short circuit case. In addition, it shows the electric field inside the two depletion regions. Excess carriers' concentrations and their current densities are derived in the three quasi-neutral regions. No need to derive them in the depletion region as its width is very small due to high doping concentration for both n^+ emitter and p^+ base. Moreover, it is assumed that there is no recombination inside the depletion region.

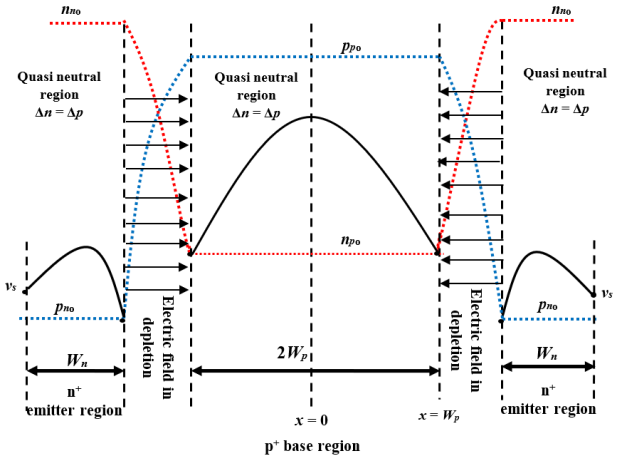

FIGURE 3. Distribution of excess carrier's concentrations inside npn structure in short circuit case.

Thus, all light-generated carriers are assumed to be separated and collected.

Considering the boundary conditions, there are two points. Firstly, the centerline is taken at $x = 0$. At this point, it is assumed that excess electrons distribution is maximum; thus, its gradient is zero. Secondly, at $x = W_p$. Being at the junction boundary, it is the interesting point at which the electron current must be derived. The junction boundary is assumed to be ideal Ohmic contact in short circuit case; thus, the excess electron concentrations is zero at $x = W_p$.

Solving equation (3) leads to finding the excess electron concentration as follows,

$$\Delta n(x) = Ae^{-\frac{x}{L_n}} + Be^{\frac{x}{L_n}} + \tau_n g_{ph}(y, \lambda) \tag{7}$$

Before obtaining the coefficients, A and B, it is important to indicate that, $g_{ph}(y, \lambda)$ is assumed to be constant with respect to x. It is only a function of y and λ. Also, as the p^+ base has a uniform doping, τ_n is considered to be constant with respect to x and y. The boundary conditions are as follows:

- Boundary condition 1, at $x = 0$, Δn is assumed to be maximum.
- Boundary condition 2, at $x = W_p$, as the structure is short-circuited, thus there is no excess at junction boundary, so $\Delta n = 0$.

Then, we can find A and B:

$$A = B = -\frac{\tau_n g_{ph}(y, \lambda)}{2\cosh\left(\frac{W_p}{L_n}\right)} \tag{8}$$

Finally, the excess electron concentration for the short circuit case, $\Delta n(x)$, as a function of x is determined by:

$$\Delta n(x) = \frac{\tau_n g_{ph}(y, \lambda)\left[1 - \cosh(x/L_n)\right]}{\cosh\left(W_p/L_n\right)} \tag{9}$$

From the expression of $\Delta n(x)$, it is obvious that the excess electron concentration is a cosh function. This confirms the assumption that the excess electron concentration is

maximum at $x = 0$. As there is no electric field in the quasi neutral regions, due to the short circuit case, there is only electron diffusion current. As well known, the diffusion current component is calculated at W_p, the edge of the junction at which carriers separated and collected. So, this current is derived as follows,

$$J_n|_{W_p} = qD_n \frac{\delta \Delta n}{\delta x}\bigg|_{W_p} \tag{10}$$

By differentiating Δn w.r.t x and substituting in equation (10), one gets:

$$J_n = qD_n \tau_n g_{ph}(y, \lambda) L_n \tanh\left(\frac{W_p}{L_n}\right) \tag{11}$$

As stated before, the relation between the electron diffusion length, L_n, and the p^+ base width, W_p, affects the structure performance because of bulk recombination. Thus, there are two important extreme cases relate L_n and W_p. These two cases are:

Case 1: at $W_p \ll L_n$, equation (11) can be reduced to:

$$J_n = qg_{ph}(y, \lambda) W_p \tag{12}$$

From equation (12), it is obvious that when W_p is smaller than L_n, the current reaches its maximum value. This fact is physically confirmed. It means that as long as W_p is smaller than L_n, almost all the light generated carriers are separated and collected by the junction. Thus, the effect of bulk recombination is very low. This causes the current to reach a value near its maximum.

Case 2: $W_p \gg L_n$, equation (11) can be reduced to:

$$J_n = qD_n \tau_n g_{ph}(y, \lambda) L_n \tag{13}$$

From equation (13), it is obvious that when W_p is greater than L_n, the current reaches its minimum value. This fact is physically confirmed. It means that as long as W_p greater than L_n, the bulk recombination dominates the separation and collection of the light generated carriers by the junctions. In addition, the top n^+ planar cell becomes more effective than sidewall. As the top n^+ is a non-useful planar cell because of high doping of p^+ base, thus the primary structure responsible for the collection of long wavelengths, sidewall junctions, becomes ineffective. These are the reasons that the current reaches its minimum values when W_p higher than L_n.

Now, we are going to find an expression for the hole current density inside the n^+ region. When solving in the n^+ emitter region, there are two points that must be considered. These points determine the required boundary conditions for completing the solution. Firstly, at $x = 0$ (at the sidewall surface of n^+ emitter region), it is assumed that there is a surface recombination velocity. It means that there is a loss in the hole current due to surface recombination. The second point is $x = W_n$(at the junction boundary), at which the hole current density must be derived. As the junction is short-circuited, thus the hole concentration is zero at $x = W_n$.

Solving equation (5)

$$\Delta p(x) = Ae^{-\frac{x}{L_p}} + Be^{\frac{x}{L_p}} + \tau_p g_{ph}(y, \lambda) \tag{14}$$

Although the doping of n^+ emitter region is non-uniform, it has a profile because of diffusion, in this analytical model, pn junctions are assumed to change abruptly to simplify the model solution. Thus, doping is assumed to be uniform in both n^+ emitter and p^+ base regions. Thus, τ_p is assumed to be constant with respect to x and y. the boundary conditions are as follows:

- Boundary condition 1, at $x = 0$, $v = v_s$, thus, $qD_p \delta \Delta p/\delta x\big|_{x=0} = q\Delta p(0) v_s$; where $qD_p \delta \Delta p/\delta x$ is a loss current due to recombining contacts at sidewalls.
- Boundary condition 2, at $x = W_n$, as the structure is short-circuited, thus there is no excess at junction boundary, so $\Delta p(x) = 0$

After some mathematical simplifications, A and B are found:

$$A = \left[\frac{\left(-g_{ph}(y, \lambda) \tau_p e^{-\frac{W_n}{L_p}}\right)}{\left(\frac{D_p}{V_s L_p - 1}\right)}\right] \times \left[\frac{(D_p - V_s L_p)}{\left((D_p - V_s L_p) \times e^{-\frac{W_n}{L_p}} + (D_p + V_s L_p) \times e^{\frac{W_n}{L_p}}\right)}\right] \tag{15a}$$

$$B = \left[\frac{\left(-g_{ph}(y, \lambda) \tau_p e^{\frac{W_n}{L_p}}\right)}{\left(\frac{D_p}{V_s L_p - 1}\right)}\right] \times \left[\frac{(D_p - V_s L_p)}{\left((D_p - V_s L_p) \times e^{-\frac{W_n}{L_p}} + (D_p + V_s L_p) \times e^{\frac{W_n}{L_p}}\right)}\right] \times \left[\left(\frac{(D_p + V_s L_p)}{(D_p - V_s L_p)}\right) + \left(\frac{(-g_{ph}(y, \lambda) \tau_p)}{(D_p - V_s L_p)}\right)\right] \tag{15b}$$

Then, we can find that:

$$J_p = \frac{qD_p}{L_p}\left[Ae^{\frac{-W_n}{L_p}} - Be^{\frac{W_n}{L_p}}\right] \tag{16}$$

In the n^+ emitter region, it is not essential to get the expressions for hole concentrations and its current density in terms of their diffusion length. The reason is that the n^+ emitter is too narrow with respect to the p^+ base region. Thus, the bulk recombination in n^+ emitter is not the main issue for its design, but it is the case for the p^+ base. The doping and sidewall surface treatments are most important in n^+ emitter design. However, the resulting expression of hole concentrations and current density depends on the length of the hole diffusion L_p.

The overall structure performance at short circuit is the summation of J_n and J_p, equations (11) and (16), multiplied by two, thus $J_{sc} = 2\times(J_n + J_p)$.

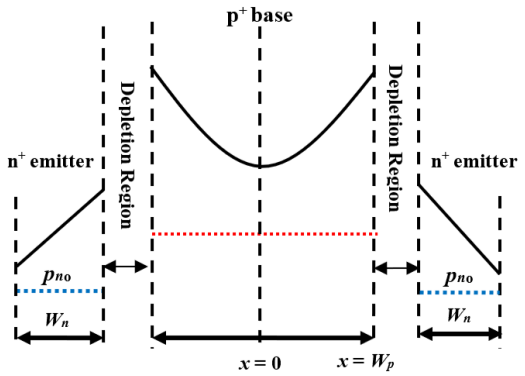

FIGURE 4. Distribution of excess carrier's concentrations in dark case.

2) DERIVATION OF EXCESS CARRIERS' CONCENTRATIONS IN DARK CASE

Fig. 4 shows the distribution of excess carriers inside the three quasi neutral regions of the structure, in the dark case. It is clear that there are excess carriers on the junction boundaries because of the law of pn junction. The n^+ emitter sidewall surfaces are assumed to be passivated using SiO_2, such as in the short circuit case.

In the dark case, there is no photogeneration rate, thus $g_{ph} = 0$. First, we determine the electron concentration and their current density inside the p^+ base.

$$\Delta n\,(x) = Ae^{-\frac{x}{L_n}} + Be^{\frac{x}{L_n}} \tag{17}$$

The boundary conditions, in this case, are given below:

- Boundary condition 1, at $x = W_p$, Δn is determined from the law of pn junction, thus $\Delta n\,(W_p) = n_{po}\left(e^{\frac{V}{V_T}} - 1\right)$
- Boundary condition 2, at $x = 0$, $\Delta n(x)$ is minimum thus $\delta\Delta n/\delta x$ is zero.

Then, we can find that:

$$A = B = \frac{\Delta n\,(W_p)}{2\cosh\left(\frac{W_p}{L_n}\right)} \tag{18}$$

Substituting from equation (18) into (17):

$$\Delta n\,(x) = \left[\frac{\Delta n\,(W_p)}{2\cosh\left(\frac{W_p}{L_n}\right)}\right]\cosh\left(\frac{x}{L_n}\right) \tag{19}$$

The diffusion current component is:

$$J_n|_{W_p} = qD_n\delta\Delta n/\delta x|_{W_p}$$
$$\Rightarrow J_n = \frac{qD_n}{L_n}\tanh\left(\frac{W_p}{L_n}\right)\left[n_{po}(e^{\frac{V}{V_T}} - 1)\right] \tag{20}$$

where $n_{po} = \frac{n_{ie}^2}{N_d}$, and $n_{ie} = n_{io}e^{\frac{-\Delta E_g}{kT}}$.

ΔE_g is the band shift attributable to bandgap narrowing resulting from high doping effect, k is Boltzmann's constant, and T is the absolute temperature. As a highly doped p^+ substrate is used, the bandgap narrowing effect must be included in the model to take the high doping effects into consideration [22]. In addition, as long as p^+ base doping, N_d, increases, n_{po} decreases, thus, the dark current decreases, which is good as it is considered a source of losses in solar cell. But at a certain doping level, the effect of the bandgap narrowing is dominated. It means, it starts to decrease E_g; thus, the dark current increases. As a result, the open circuit voltage of the cell decreases. Thus, the overall structure performance shows that the conversion efficiency decreases. So, there must be an optimum doping for p^+ base at which the effect of bandgap narrowing does not severely degrade the structure performance.

By the same way, we can get the hole concentration and its current density inside the n^+ emitter region in dark case:

$$\Delta p\,(x) = Ae^{-\frac{x}{L_p}} + Be^{\frac{x}{L_p}} \tag{21}$$

- Boundary condition 1, at $x = W_n$, $\Delta p\,(W_n) = p_{no}\left(e^{\frac{V}{V_T}} - 1\right)$, from the law of pn junction.
- Boundary condition 2, at $x = 0$, $D_p\delta\Delta p/\delta x\big|_{x=0} = q\Delta p\,(0)\,v_s$

Then,

$$A = \left[\frac{(D_p - V_sL_p)}{(D_p + V_sL_p)}\right] \times B \tag{22a}$$

$$B = \left[\frac{\left(\Delta p\,(W_n) \times (D_p + V_sL_p)\right)}{\left((D_p + V_sL_p) \times e^{\frac{W_n}{L_p}} + (D_p - V_sL_p) \times e^{\frac{-W_n}{L_p}}\right)}\right] \tag{22b}$$

Now, J_p can be derived at $x = W_n$ as follows:

$$J_p = -qD_p\delta\Delta p/\delta x\big|_{x=W_n}$$
$$\Rightarrow J_p = -\frac{qD_p}{L_p}\left[Ae^{\frac{-W_n}{L_p}} - Be^{\frac{W_n}{L_p}}\right] \tag{23}$$

The overall structure performance at dark is the summation of J_n and J_p, equations (20) and (23), multiplied by two, thus $J_{\text{dark}} = 2\times(J_n + J_p)$.

The total performance of the vertical structure is the summation of the short circuit and the dark current densities, thus, $J_{\text{total}} = J_{\text{sc}} + J_{\text{dark}}$. The total npn structure performance = the total performance of the top planar structure + The total performance of vertical structure.

B. THE OPTICAL MODEL FOR THE NPN STRUCTURE

INPUT SOLAR RADIATION SPECTRUM

The photogeneration rate g_{ph} is given by:

$$g_{ph}\,(y, \lambda) = \alpha d\lambda I\,(y) \tag{24}$$

where α is the absorption coefficient. The photon flux $I(y)$, taking the effect of back-reflected photons into consideration, is expressed as follows:

$$I\,(y) = I_oe^{-\alpha y} + I_oe^{-\alpha(2t\text{-}y)} \tag{25}$$

All top surface treatments and the description of the optical input for the npn structure is included in I_o, where $I_o = F(1 - R)$. Where F is the input solar radiation spectrum and R is the silicon reflection coefficient. The input solar radiation spectrum is assumed to be AM1.5. Also, F, R and α have tables for their values with each wavelength [24]–[26].

IV. MODEL VALIDATION VS TCAD SIMULATION

In this section, the developed analytical model is verified using SILVACO TCAD device simulator. The model is implemented in MATLAB. The results from the model and that from SILVACO are compared to emphasize the visibility of the analytical model. The presented results include both the structure electrical IV and optical characteristics. The main electrical parameters are extracted like the open circuit voltage (V_{oc}), short circuit current density (J_{sc}), fill factor (FF) and conversion efficiency (η_c). Regarding the optical performance, the quantum efficiency and spectral response are extracted.

To develop the comparison, a case study for the npn structure physical and technological parameters is chosen. It is not the optimized case of the structure; however, it is just used to evaluate and verify the analytical model numerically. In this case study, the parameters are assumed as follows. The p^+ base doping is chosen to be 10^{18} cm^{-3}. For this doping, the electron diffusion length, L_n, is assumed to be 10 μm. W_p must be smaller than L_n, in order to overcome bulk recombination and increase short circuit current; thus, W_p is chosen to be 8 μm. The electron lifetime, τ_{no}, is chosen to be 1 μsec [27]. Thus, at doping 10^{18} cm^{-3}, τ_n equals approximately to 0.05 μsec. This is a worst-case value for electron lifetime as the actual lifetime may be greater than the assumed value in this case study.

Concerning n^+ emitter parameters, it should be a good emitter, to enhance its injection efficiency. Thus, its doping is chosen to be high, 2×10^{20} cm^{-3}. At this doping, L_p is 0.15 μm [28]. Actually, the bulk recombination is not the major effect concerning n^+ emitter design because it is narrow with respect to W_p. To be a good emitter, its width has to be slightly wide, greater than L_p, to decrease the reverse saturation current. The bulk recombination is not greatly effective at this width. Thus, W_n is chosen to be 0.19 μm. the hole lifetime, τ_{po}, is chosen to be 1 μsec. Thus, at doping 2×10^{20} cm^{-3}, τ_p equals to 0.24 nsec [27]. For the top n^+ pn junction, its doping is chosen to be 5×10^{19} cm^{-3}. Its thickness is chosen to be 0.1 μm. It means that the structure is ultraviolet collector.

Concerning the structure thickness, t, it is chosen to be 80 μm. The reason is that, 80 μm wafers are low cost solar wafers used for planar solar cells with doping 10^{17} cm^{-3}. As the npn structure uses higher doping, thus the cost of the 80 μm low cost solar cell wafers becomes lower [29].

The third dimension of the structure, L, is assumed to be 1 μm. The effects of the structure notches are included in the model. Thus, the top structure exposed area to the input radiation spectrum, which is used to calculate its short circuit current density, J_{sc}, equals to [(2 W_p + notch width)× L]. The technological and physical parameters for the case study are summarized in Table 2.

TABLE 2. Technological and physical parameters.

Parameter	Value
p^+ base doping	10^{18} cm^{-3}
p^+ (Base) Base thickness ($2W_p$)	16 μm
Top n^+ Thickness	0.1 μm
Top n^+ Doping	5×10^{19} cm^{-3}
SiO_2Thickness	0.1 μm
Emitter thickness (W_n)	0.18 μm
Emitter Doping	2×10^{20} cm^{-3}
Cell thickness (t)	80 μm
L	1 μm

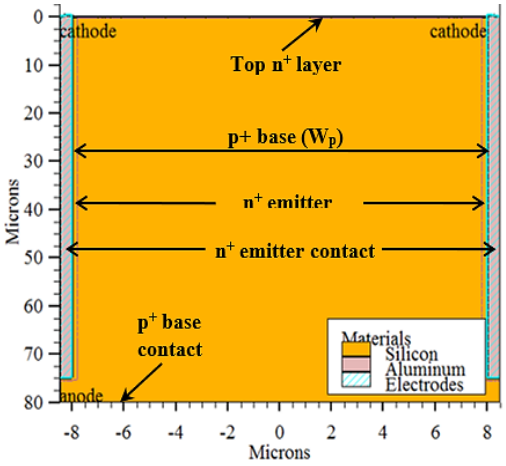

FIGURE 5. The npn structure using Athena process simulator.

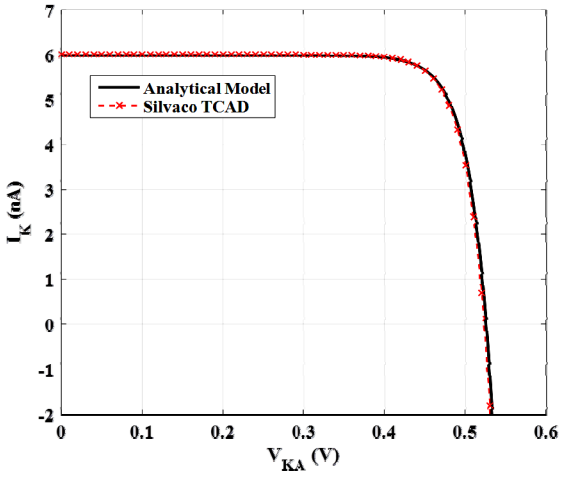

FIGURE 6. Comparison between the npn structure IV Characteristic from both MATLAB model and SILVACO.

Now, the case study is applied to both the analytical model and SILVACO TCAD. For SILVACO simulations, we start by a process simulator ATHENA to define the structure. Fig. 5 shows the specified structure. All the physical and technological parameters are taken to be the same as

TABLE 3. Comparison between the evaluated electrical performance parameters.

Parameter	Analytical Model	TCAD
I_{sc} (nA)	5.98	6.01
J_{sc} (mA/cm^2)	35.19	35.35
V_{oc} (V)	0.526	0.523
FF (%)	80.95	80.80
η_c (%)	11.73	11.7

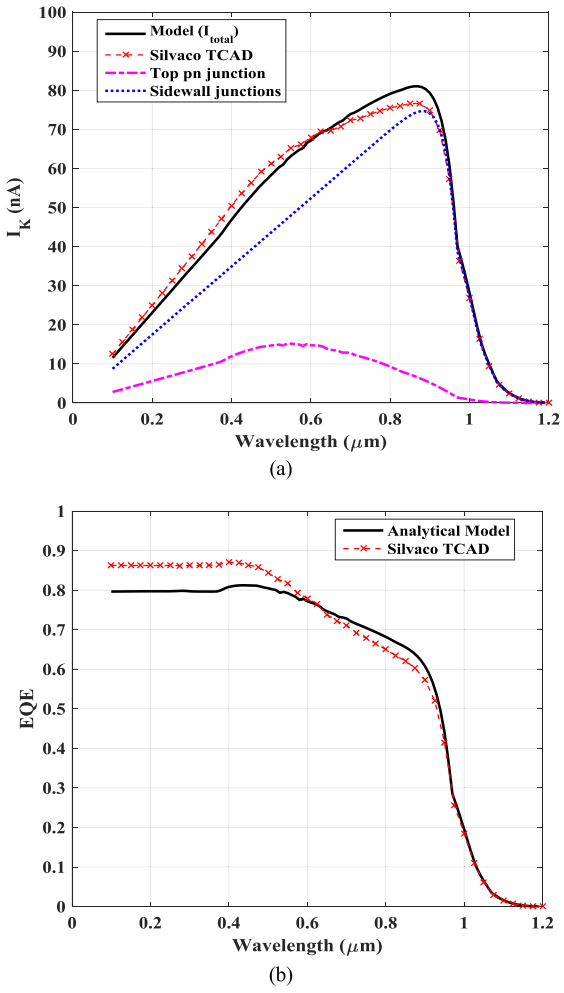

FIGURE 7. Comparison of optical characteristics: SILVACO vs Model (a) spectral response and (b) external quantum efficiency.

mentioned above. The sidewall surfaces of the n+ emitter are passivated using SiO_2. Thus, the n^+ emitter surface has low surface recombination velocity. The device simulations are done using the device simulator ATLAS.

Fig. 6 shows the npn structure evaluated IV characteristics. As shown in the figure, the IV characteristics have a good square characteristic, which means that the structure fill factor is high. Also, the figure indicates that the analytical model is capable of evaluating the IV characteristics correctly compared to the full solution of the drift diffusion model accomplished by TCAD simulations.

Further, Table 3 summarizes the comparison between the evaluated electrical performance parameters of the case study using the presented model and SILVACO. The comparison from Table 3 confirms the electrical validation of our model vs TCAD simulations.

Finally, Fig. 7 shows the comparison between the spectral response (Fig. 7(a)) and the external quantum efficiency (Fig. 7(b)) of the case study using both the developed model results and TCAD simulations. The important data taken from these two figures is that the structure responds to the ultraviolet part of the input radiation spectrum. This emphasizes that the top pn junction is designed to be ultraviolet collector. The structure often reacts well to the rest of the input range of solar radiation, the long wavelength till the silicon cutoff wavelength 1.1 μm. The vertical pn junction functions well as a long wavelength collector.

In addition, returning to Fig. 7(a), it is clear that the spectral response of the top n^+ region is nearly negligible compared to the spectral response of the two vertical side wall junctions. These results confirm the importance of using the vertical junction for overcoming the effect of short carriers diffusion length of the low cost highly doped silicon wafer. Also, it emphasizes that the top n+ region is responsible for the collection of the ultraviolet part of the input solar radiation spectrum.

V. CONCLUSION

In this work, an analytical model is developed for a proposed low-cost npn solar cell whose operation based on the concept of vertical generation and lateral light carriers collection. The main objective of this model is to achieve a transparent solution for the structure performance. This solution paves the way for optimizing the physical and technological parameters of the structure. Thus, the structure performance can be enhanced. The analytical model electrical and optical performance is verified using SILVACO device simulator. A comparison between both the analytical model and SILVACO is carried out to confirm the validation of the model. Although our model is based on some approximations, it gives reasonable accuracy with fewer simulation times. Also, it gives a figure of merits of the technological parameters' values. Based on the transparent result of the npn structure analytical model, the optimum design of its physical and technological parameters will be investigated. Thus, npn structure performance are going to be enhanced.

For a simple case study, an npn cell efficiency of above 11% is achieved. Although the obtained efficiency is lower than recent fabricated crystalline silicon solar cells, the efficiency could be boosted by inspecting some design ideas such as lifetime improvement and flipping the cell such as to prevent shadowing effects.

Moreover, in the current presented model, abrupt junction approximation is utilized. In our future work, we will consider the improvement of the model to include doping profiles

resulting from real fabrication processes. Also, more design ideas will be discussed to increase the efficiency of this promising low-cost structure. By improving the analytical model, reliable optimization processes could be performed easily in order to enhance the npn cell performance, which would become a low-cost solar cell with high efficiency. This will make it to compete with the commercially available cells.

REFERENCES

[1] E. Scalise, "Tailoring the electronic properties of semiconducting nanocrystal-solids," *Semicond. Sci. Technol.*, vol. 35, no. 1, p. 13001, 2019, doi: 10.1088/1361-6641/ab52e0.

[2] M. M. Salah, K. M. Hassan, M. Abouelatta, and A. Shaker, "A comparative study of different ETMs in perovskite solar cell with inorganic copper iodide as HTM," *Optik*, vol. 178, pp. 958–963, Feb. 2019, doi: 10.1016/j.ijleo.2018.10.052.

[3] O. A. M. Abdelraouf, A. Shaker, and N. K. Allam, "Novel design of plasmonic and dielectric antireflection coatings to enhance the efficiency of perovskite solar cells," *Sol. Energy*, vol. 174, pp. 803–814, Nov. 2018, doi: 10.1016/j.solener.2018.09.066.

[4] Z. Shi, X. Wang, Y. Sun, Y. Li, and L. Zhang, "Interlayer coupling in two-dimensional semiconductor materials," *Semicond. Sci. Technol.*, vol. 33, no. 9, p. 93001, 2018, doi: 10.1088/1361-6641/aad6c3.

[5] A. Ebong, M. Hilali, V. Upadhyaya, S. Rounsaville, I. Ebong, and A. Rohatgi, "High efficiency screen-printed planar solar cells on single crystalline silicon materials," in *Proc. Conf. Rec. 31st IEEE Photovoltaic Specialists Conf.*, Jan. 2005, pp. 1173–1176, doi: 10.1109/PVSC.2005.1488347.

[6] S. Peters, C. Ballif, D. Borchert, R. Schindler, W. Warta, and G. Willeke, "Record fast thermal processing of 17.5 efficient silicon solar cells," *Semicond. Sci. Technol.*, vol. 17, no. 7, pp. 677–681, Jul. 2002, doi: 10.1088/0268-1242/17/7/307.

[7] I. Hamammu and K. Ibrahim, "Low cost fabrication for high efficiency monocrystalline silicon solar cells," in *Proc. 3rd World Conf. Photovoltaic Energy Convers.*, vol. 2, 2003, pp. 1519–1520.

[8] K. Murukesan and N. R. Mavilla, "Towards fabrication of low cost high efficiency C-Si solar cells: Progress and optimization using TCAD simulation study," in *Proc. 38th IEEE Photovoltaic Specialists Conf.*, Jun. 2012, pp. 2218–2222, doi: 10.1109/PVSC.2012.6318037.

[9] L. J. Geerligs, I. G. Romijn, A. R. Burgers, N. Guillevin, A. W. Weeber, J. H. Bultman, H. Wang, F. Lang, W. Zhao, G. Li, Z. Hu, J. Xiong, and A. Vlooswijk, "Progress in low-cost n-type silicon solar cell technology," in *Proc. 38th IEEE Photovoltaic Spec. Conf.*, Jun. 2012, pp. 1701–1704, doi: 10.1109/PVSC.2012.6317923.

[10] B. M. Kayes, H. A. Atwater, and N. S. Lewis, "Comparison of the device physics principles of planar and radial p-n junction nanorod solar cells," *J. Appl. Phys.*, vol. 97, no. 11, Jun. 2005, Art. no. 114302, doi: 10.1063/1.1901835.

[11] E. C. Garnett and P. Yang, "Silicon nanowire radial p–n junction solar cells," *J. Amer. Chem. Soc.*, vol. 130, no. 29, pp. 9224–9225, Jul. 2008, doi: 10.1021/ja8032907.

[12] M. S. Salem, A. Shaker, M. Abouelatta, and A. Zekry, "Effect of base width variation on the performance of a proposed ultraviolet low cost high efficiency solar cell structure," in *Proc. 38th IEEE Photovoltaic Spec. Conf.*, Jun. 2012, pp. 000775–000777, doi: 10.1109/PVSC.2012.6317718.

[13] M. S. Salem, A. Zekry, A. Shaker, M. Abouelatta, and T. M. Abdolkader, "Performance enhancement of a proposed solar cell microstructure based on heavily doped silicon wafers," *Semicond. Sci. Technol.*, vol. 34, no. 3, p. 35012, 2019, doi: 10.1088/1361-6641/ab0078.

[14] M. D. Kelzenberg, D. B. Turner-Evans, B. M. Kayes, M. A. Filler, M. C. Putnam, N. S. Lewis, and H. A. Atwater, "Single-nanowire Si solar cells," in *Proc. 33rd IEEE Photovoltaic Spec. Conf.*, May 2008, pp. 1–6, doi: 10.1109/PVSC.2008.4922736.

[15] M. C. Putnam, "Si microwire-array solar cells," *Energy Environ. Sci.*, vol. 3, no. 8, pp. 1037–1041, 2010, doi: 10.1039/C0EE00014K.

[16] H. Bashiri, M. A. Karami, and S. M. Nejad, "An analytical approach for modeling of high-efficiency crystalline silicon solar cells with homo–hetero junctions," *Mater. Sci. Semicond. Process.*, vol. 111, Jun. 2020, Art. no. 104960, doi: 10.1016/j.mssp.2020.104960.

[17] N. M. Ali, N. K. Allam, A. M. Abdel Haleem, and N. H. Rafat, "Analytical modeling of the radial pn junction nanowire solar cells," *J. Appl. Phys.*, vol. 116, no. 2, p. 24308, Jul. 2014, doi: 10.1063/1.4886596.

[18] NREL. (2017). *Best Research-Cell Efficiencies*. [Online]. Available: https://www.nrel.gov/pv/assets/images/efficiency-chart.png

[19] P. K, U. Govindarajan, V. K. Ramachandaramurthy, S. O. S. T, and B. Jeevarathinam, "Integrating solar photovoltaic energy conversion systems into industrial and commercial electrical energy utilization—A survey," *J. Ind. Inf. Integr.*, vol. 10, pp. 39–54, Jun. 2018, doi: 10.1016/j.jii.2018.01.003.

[20] K. Balasundaram, J. S. Sadhu, J. C. Shin, B. Azeredo, D. Chanda, M. Malik, K. Hsu, J. A. Rogers, P. Ferreira, S. Sinha, and X. Li, "Porosity control in metal-assisted chemical etching of degenerately doped silicon nanowires," *Nanotechnology*, vol. 23, no. 30, Aug. 2012, Art. no. 305304, doi: 10.1088/0957-4484/23/30/305304.

[21] R. T. S. Rein, J. Broisch, W. Kwapil, G. Emanuel, I. Reis, A.-K. Soiland, and S. Grandum, "Cz-silicon wafers and solar cells from compensated solar-grade silicon feedstock: Potential and challenges," in *Proc. 25th Eur. Photovolt. Sol. Energy Conf. Exhib./5th World Conf. Photovolt. Energy Convers.*, Valencia, Spain, Sep. 2010, pp. 1186–1194, doi: 10.4229/25thEUPVSEC2010-2BO.1.2.

[22] S. M. Sze and K. K. Ng, *Physics of Semiconductor Devices*. Hoboken, NJ, USA: Wiley, 2006.

[23] A. Zekry, A. Shaker, and M. Salem, "Solar cells and arrays: Principles, analysis, and design," in *Advances in Renewable Energies and Power Technologies*. Amsterdam, The Netherlands: Elsevier, 2018, pp. 3–56.

[24] R. Santbergen and R. J. C. van Zolingen, "The absorption factor of crystalline silicon PV cells: A numerical and experimental study," *Sol. Energy Mater. Sol. Cells*, vol. 92, no. 4, pp. 432–444, Apr. 2008, doi: 10.1016/j.solmat.2007.10.005.

[25] K. Chen, J. Zha, F. Hu, X. Ye, S. Zou, V. Vähänissi, J. M. Pearce, H. Savin, and X. Su, "MACE nano-texture process applicable for both single- and multi-crystalline diamond-wire sawn Si solar cells," *Sol. Energy Mater. Sol. Cells*, vol. 191, pp. 1–8, Mar. 2019, doi: 10.1016/j.solmat.2018.10.015.

[26] M. A. Green and M. J. Keevers, "Optical properties of intrinsic silicon at 300 k," *Prog. Photovolt., Res. Appl.*, vol. 3, no. 3, pp. 189–192, 1995, doi: 10.1002/pip.4670030303.

[27] A. Zekry, "The dependence of diffusion length, lifetime and emitter Gummel-number on temperature and doping," *Archiv Elektrotechnik*, vol. 75, no. 2, pp. 147–154, Mar. 1992, doi: 10.1007/BF01577633.

[28] J. A. del Alamo and R. M. Swanson, "Modelling of minority-carrier transport in heavily doped silicon emitters," *Solid-State Electron.*, vol. 30, no. 11, pp. 1127–1136, Nov. 1987, doi: 10.1016/0038-1101(87)90077-3.

[29] A. Goodrich, P. Hacke, Q. Wang, B. Sopori, R. Margolis, T. L. James, and M. Woodhouse, "A wafer-based monocrystalline silicon photovoltaics road map: Utilizing known technology improvement opportunities for further reductions in manufacturing costs," *Sol. Energy Mater. Sol. Cells*, vol. 114, pp. 110–135, Jul. 2013, doi: 10.1016/j.solmat.2013.01.030.